Blending Effects on Polymorphic Crystallization of Poly(L-lactide)

Pengju Pan, Zhichao Liang, Bo Zhu, Tungalag Dong, and Yoshio Inoue*

Department of Biomolecular Engineering, Tokyo Institute of Technology, 4259-B-55 Nagatsuta, Midori-ku, Yokohama 226-8501, Japan

Received November 7, 2008; Revised Manuscript Received January 30, 2009

ABSTRACT: The effects of miscible blending on the crystallization kinetics and crystalline structure of poly(L-lactide) (PLLA) were investigated by differential scanning calorimetry (DSC), polarized optical microscopy (POM), Fourier transform infrared (FTIR) spectroscopy, and wide-angle X-ray diffraction (WAXD). It was confirmed that the blends of PLLA and poly(D,L-lactide) (PDLLA) are miscible at all compositions. Due to the dilution effect, the crystallization of PLLA was hindered with the presence of PDLLA. The PLLA/PDLLA blends show the irregular or ring-banded spherulites. The polymorphic behavior of PLLA is influenced by the miscible blending with PDLLA. FTIR and WAXD data indicates that the formation of the α-form crystals of PLLA is favored in the blends. With incorporation of 50 wt % PDLLA, the critical temperature for the formation of α′- and α-form crystals decreases from ∼110 (of neat PLLA) to ∼80 °C. The factors affecting the formation of the PLLA α′- and α-form crystals were discussed from the thermodynamic and kinetic considerations. It was proposed that the formation of the metastable α′-form crystals of PLLA is kinetically preferential, while that of the thermally stable α-form crystals is thermodynamically favored. The blending effects on the crystalline structure of PLLA are ascribed to two factors, that is, the lowered equilibrium melting point and decreased crystallization rate.

Introduction

Poly(lactide) (PLA) bioplastic has been attracting considerable attention from both fundamental and practical perspectives because it can be synthesized from renewable resources and is thus environmentally and ecologically appropriate.[1,2] The attributes of biodegradability, biocompatibility, good mechanical properties, and versatile fabrication processes make it a promising material for biomedical applications such as implant materials, surgical suture, and controlled drug delivery systems, as well as for the conventional applications where common thermoplastics are employed.[1,2] Due to the presence of a chiral carbon in the skeletal chain, PLA has two stereoregular enantiomers, poly(L-lactide) (PLLA) and poly(D-lactide) (PDLA). The polymerization of racemic lactide (or lactic acid) or *meso*-lactide results in the formation of atactic poly(D,L-lactide) (PDLLA).

The common enantiomer of PLA, that is, PLLA, crystallizes in α-,[3,4] β-,[5] or γ-form[6] crystals, depending on the preparation conditions. The most common modification, α-form, characterized by two antiparallel left-handed helical chains in a 10_3 (or distorted 10_3) conformation packed in an orthorhombic (or pseudo-orthorhombic) unit cell, is generally developed from the normal cold, melt, or solution crystallization.[3,4] Recently, a limit-disordered modification, designated as α′-form, has been proposed for the PLLA samples cold- or melt-crystallized at low crystallization temperature (T_c < 100 °C) by several research groups, compared to the normal α-form crystals crystallized at high T_c (>120 °C).[7−11] As we know, PLLA is usually molded at 100−120 °C in the industrial melt-processing, because of the fast crystallization rate over this temperature region.[2] Over the T_c region of 100−120 °C, the α′ + α mixture crystals of PLLA are formed,[7−10] indicating that the PLLA α′-form crystals indeed exist widely in many PLLA-based products. Therefore, studies on the crystalline structure, physical properties, and generation mechanism of the PLLA α′-form crystals are of fundamental importance from the perspective of practical applications. Although it has been reported that the PLLA α′- and α-form crystals have different crystallization kinetics[8,12] and thermodynamic stability,[8−11] the kinetic and thermodynamic factors affecting the formation of the α′-form crystals still remain unclear.

A variety of physical properties such as mechanical and electrical properties of polymorphic polymers considerably depend on the crystalline structure.[13] As far as the biodegradable polyesters are concerned, their biodegradability is also influenced by the crystal modifications.[14] For this reason, regulating the crystal modifications of polymorphic polymers via changing the crystallization or processing conditions is an important approach to tailor the final properties of polymeric materials. It has been reported that, aside from temperature and stress, the crystal modifications of a polymorphic polymer can be manipulated by many methods such as the addition of nucleating agents,[15,16] epitaxial crystallization on the surfaces of other substances,[6,17] incorporation of comonomeric units,[13] and polymer blending.[18−20] Among them, the polymer blending is one of the most convenient methods in the industrial processing and a widely used way to develop the new materials with better performances. At present, the miscible blending has been successfully utilized to control the polymorphic behavior of syndiotactic polystyrene (s-PS). In the blends of s-PS with some miscible components such as atactic polystyrene (a-PS)[18] and poly(2,6-dimethyl-1,4-diphenylene oxide) (PPO),[13] the formation of the β-form crystals of s-PS is facilitated.

PLLA is known to be miscible or partially miscible with only a few counterparts such as atactic poly(3-hydroxybutyrate) (a-PHB),[21,22] poly(vinyl acetate) (PVAc),[23] poly(methyl methacrylate) (PMMA),[24] poly(vinylphenol) (PVPh),[25] poly(ethylene glycol) (PEG),[26] and PDLLA.[27,28] As we know, the glass transition temperature (T_g) is an important factor governing the crystallization behavior. Among these miscible components of PLLA, only PDLLA has the similar T_g to PLLA, and besides there is no specific interaction (e.g., hydrogen bonding) between PDLLA and PLLA. Therefore, PDLLA was selected as a model polymer in this work to study the effects of miscible blending on the polymorphic crystallization of PLLA. On the other hand, the semicrystalline PLLA has higher strength and modulus and relatively slower degradation rate, making it an ideal biomaterial for load bearing devices. In contrast, due to the amorphous nature, PDLLA shows weaker mechanical properties and faster

* To whom correspondence should be addressed. Telephone: +81-45-924-5794. Fax: +81-45-924-5827. E-mail: inoue.y.af@m.titech.ac.jp.

10.1021/ma8024943 CCC: $40.75 © 2009 American Chemical Society
Published on Web 04/14/2009

degradation rate, making it a preferred candidate for developing the drug delivery vehicles and as the low strength scaffolding material for tissue regeneration.[1] Consequently, blending PLLA and PDLLA can balance the mechanical properties and degradation rate and attain the biomaterials with the controllable and improved performances.

Generally, the commercial PLLA is not completely stereoregular and usually contains 0.5−5 mol % D-lactic acid units, depending on the monomer purity and synthesis methods (e.g., ring-opening polymerization or polycondensation). Several authors[29−33] have investigated the effects of stereoregularity and stereodefects on the crystallization kinetics, morphology, and solid-state structure of PLLA. However, to our knowledge, the correlation between stereoregularity and the polymorphic behavior (i.e., formation of α′- and α-form crystals) of PLLA has been unexplored. In the melt-crystallization process, the plot of spherulite growth rate (G) vs T_c for PLLA with high stereoregularity deviates from the typical bell-shaped curve and shows two maxima,[8,12,32,33] ascribing to the different growth kinetics of α′- and α-form crystals. Interestingly, with the incorporation of D-lactic acid units in PLLA chain, the typical bell-shaped curve of G vs T_c was observed in the poly(L-lactide-*co*-D-lactide) copolymers.[32,33] This suggests that the stereoregularity of PLLA is likely to be a significant factor affecting the formation of α′- and α-form crystals. Therefore, study on the polymorphic behavior of PLLA/PDLLA blends will shed light on the solid-state structure of the commercial PLLA materials. Moreover, the thermodynamic and kinetic factors of crystallization will change upon blending, making it possible to elucidate the origin of polymorphism in PLLA.

The present study has 2-fold objectives, that is, (i) manipulating the crystal modifications of PLLA by the miscible polymer blending, and (ii) studying the thermodynamic and kinetic factors affecting the formation of the α′- and α-form crystals of PLLA. In this work, the crystallization kinetics, spherulite morphology, and crystalline structure of the PLLA/PDLLA blends with various compositions were investigated and compared with the neat PLLA. The effects of blend composition and crystallization conditions on the polymorphic behavior of PLLA were analyzed. Besides, the factors that influence the formation of the PLLA α′- and α-form crystals were discussed from the thermodynamic and kinetic considerations.

Experimental Section

Materials. PLLA sample (M_n = 94 kg/mol, M_w/M_n = 1.52), consisted of ∼0.5 mol % D-lactic acid units, was kindly supplied by Unitika Co. Ltd. (Kyoto, Japan). Poly(D,L-lactide) (PDLLA) sample (M_n = 46 kg/mol, M_w/M_n = 1.91), a completely noncrystallizable polymer that was prepared by the ring-opening polymerization of *meso*-lactide (D,L-lactide) and consisted of the equimolar D- and L-lactic acid units, was kindly supplied by Shimadzu Co. (Kyoto, Japan). Before use, the samples were purified by precipitation into ethanol from chloroform solution and then were dried in the vacuum oven at 40 °C for 48 h.

Blend Preparation. For each blend, appropriate amounts of the PLLA and PDLLA samples were dissolved in chloroform (∼1 g/50 mL). The solutions were cast on Petri dishes, and the solvent was allowed to evaporate at room temperature. All films obtained were placed in an oven at 40 °C under vacuum for 48 h to eliminate the residual solvent. The blend is symbolized as PLLA/PDLLA *x*/*y*, where *x* and *y* represent the weight percentages of PLLA and PDLLA, respectively.

Measurements. Differential Scanning Calorimeter. The crystallization behavior of PLLA and its blends were measured on a Pyris Diamond differential scanning calorimeter (DSC) instrument (Perkin-Elmer) equipped with an intracooler 2P cooling accessory. The temperature and heat flow at different heating rates were calibrated by use of an indium standard. The measurements were conducted in a nitrogen atmosphere. The samples (∼7 mg) were weighed and sealed in an aluminum pan. In the cold-crystallization, the samples were quenched to 0 °C by a cooling rate of 100 °C/min after melting at 200 °C for 2 min. Then, they were heated to 200 at 10 °C/min for nonisothermal crystallization, or were fast heated (at 100 °C/min) to the desired temperature (T_c = 80−140 °C) for isothermal crystallization. In the case of melt-crystallization, after melting at 200 °C for 2 min, the samples were cooled to 0 at 2.5 °C/min for nonisothermal crystallization, or were quenched to the desired temperature (T_c = 80−140 °C) at 100 °C/min for isothermal crystallization. After the cold- or melt-crystallization, the samples were reheated to 200 at 10 °C/min to examine the melting behavior.

Polarized Optical Microscopy. Polarized optical microscopy (POM) observation was performed on a BX90 microscope (Olympus Co., Tokyo, Japan) equipped with a digital camera. The film samples, sandwiched by two glass slides, were heated to 200 °C and melted for 2 min in a LK-600 FTIR hot stage (Linkam Scientific Instruments) in a nitrogen atmosphere to erase the thermal history. Then, they were quickly transferred to another hot stage (Mettler FP82HT) preset to 140 °C for crystallization. The spherulite morphology was recorded after the completion of crystallization. The sizes of growing spherulites were monitored by taking micrographs at an appropriate time interval before the spherulites impinged. The averaged radial growth rate of spherulite (G) was attained from the slope of spherulite radius vs growth time plot.

FTIR Spectroscopy. FTIR measurements were performed on a FTIR-6100 spectrometer (JASCO, Japan) equipped with an IMV-4000 multichannel infrared microscope and a MCT detector worked in the transmission mode. FTIR spectra were collected with 64 scans and a resolution of 2 cm^{-1}. The sample for FTIR measurement was prepared by drop-casting a chloroform solution of PLLA or its blends on a BaF_2 window. After the majority of the solvent had evaporated, the sample was placed under vacuum at 40 °C for 48 h to remove the residual solvent. Then it was melted at 200 °C for 2 min in a LK-600 hot stage, followed by a quenching to the desired temperature (T_c = 80−140 °C) for isothermal crystallization. The melting and crystallization processes were conducted under a nitrogen atmosphere. FTIR spectra of all the crystallized samples were measured at ∼23 °C to erase the temperature effect. FTIR spectra of the amorphous samples for PLLA and blends, prepared by quenching to ∼23 °C from the melt states, were also measured under the same conditions.

Wide-Angle X-ray Diffraction. Wide-angle X-ray diffraction (WAXD) patterns were recorded on a Rigaku RU-200 (Rigaku Co., Tokyo, Japan) with Ni-filtered Cu Kα radiation (λ = 0.1542 nm), worked at 40 kV and 200 mA. The PLLA and its blend samples were first hot-pressed at 200 °C after melting for 2 min and then were transferred to a vacuum oven preset to the desired temperatures (T_c = 80−140 °C) for isothermal melt-crystallization. Finally, the WAXD patterns were recorded between Bragg angles of 5−50° at a scan rate of 1°/min under the ambient conditions. For all of the isothermally crystallized samples for DSC, FTIR and WAXD analyses, the crystallization times are approximately equal to 4 times of the peak-time (t_p) of DSC curves recorded in the isothermal crystallization process, corresponding to the time when the exotherm minimum occurs.

Results and Discussion

DSC Analysis. The cold- and melt-crystallization kinetics of PLLA/PDLLA blends were analyzed by DSC. Figure 1 shows the DSC heating curves (at 10 °C/min) of the quenched PLLA/PDLLA blend samples. In addition to the glass transition, a cold-crystallization peak at 100−150 °C and a melting peak at high temperature are observed for the neat PLLA and PLLA/PDLLA blends, except for the neat PDLLA. Figure 2 shows the DSC curves of PLLA/PDLLA blends recorded in the nonisothermal melt-crystallization (cooling at 2.5 °C/min) and subsequent heating scans at 10 °C/min. No any crystallization and melting peak is detected for neat PDLLA in all the DSC measurements,

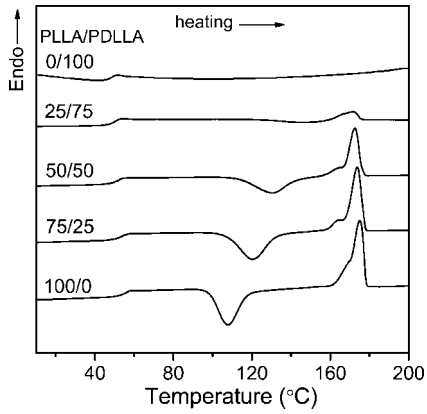

Figure 1. DSC heating curves of quenched PLLA/PDLLA blend samples recorded at the heating rate of 10 °C/min.

confirming its amorphous nature. On the basis of these DSC results, the thermal parameters of PLLA/PDLLA blends including crystallization temperature (T_c), melting enthalpy (ΔH_m), and melting point (T_m) of the cold- and melt-crystallized samples, as well as T_g of the quenched samples were evaluated, as summarized in Table 1. Figure 3 shows the peak-time (t_p) of DSC curves, corresponding to the time when the exotherm minimum occurs, for the isothermal (a) melt- and (b) cold-crystallization of PLLA/PDLLA blends. The reciprocal value of t_p (t_p^{-1}) is recognized to be proportional to the overall crystallization rate.

For the PLA samples with the similar molecular weight, as the stereoregularity decreases (e.g., as the D-lactic acid units in PLLA increases), the T_g value decreases.[34] This is attributed to the effect of stereoregularity on the helical conformation of PLA.[34,35] Besides, the PDLLA sample used in this study has a smaller molecular weight than the PLLA sample. Therefore, the PLLA and PDLLA samples show the different T_g values and the miscibility of PLLA and PDLLA can be assessed by the change of T_g. The T_g values of neat PLLA and PDLLA are 55.0 and 47.1 °C, respectively. As seen in Figure 1 and Table 1, all the blends with different compositions exhibit a single T_g that shifts to a lower temperature with an increase in the PDLLA content. From the differential DSC curves (data not shown), all the blends show the similar width of glass transition (ΔT_g), that is, ~15 °C. These results suggest the miscibility of the two blend components in the molten state.[27,28] The T_g value of this blend system is in agreement with the data calculated from Gordan-Taylor equation[36]

$$T_g = T_{g1} + kW_2(T_{g2} - T_g)/W_1 \quad (1)$$

with a k value of 1.27, where 1 and 2 represent PLLA and PDLLA, respectively. W_i is the weight fraction of component i (1 or 2), and k is an empirical adjustable parameter.

As shown in Figure 1, the cold-crystallization peak shifts to higher temperature with an increase in PDLLA composition. As seen in Figure 2b, after the nonisothermal melt-crystallization at 2.5 °C/min, a cold-crystallization peak (indicated by an arrow) appears in the PLLA/PDLLA blends during the subsequent heating process, while it is absent in the neat PLLA. Besides, as seen Figure 3, the t_p values of both the melt- and cold-crystallized samples generally increase with the PDLLA content. All these results indicate the depression of crystallization rate of PLLA upon blending with the noncrystallizable PDLLA. This is ascribed to the dilution effects of PDLLA on the PLLA component, because an extra energy is required for demixing the polymer components in the crystallization of the miscible blends and thus a higher energy is needed for the PLLA component to transport from the miscible melt to the growth front of crystal lamella.

It is noteworthy that, the t_p value of neat PLLA changes abruptly (Figure 3a) or nonmonotonously (Figure 3b) at 110−120 °C in the plot of t_p vs T_c, ascribing to the different crystallization kinetics of the PLLA α′- and α-form crystals,[8] while the discontinuous change in t_p is not observed in the blends. The transition from regime II to III can also induce the discontinuous change in t_p.[12] Therefore, the PLLA/PDLLA 75/25 blend shows larger (or comparable) t_p value than the neat PLLA at T_c = 120 and 130 °C. As seen in Figure 2a, a peak shoulder (indicated by an arrow) appears in the crystallization peak of neat PLLA, attributable to the different growth kinetics of PLLA α′- and α-form crystals,[8] while it is absent in the PLLA/PDLLA blends. All these results of nonisothermal and isothermal crystallization kinetics suggest that the polymorphic behavior of PLLA/PDLLA blends might differ from that of neat PLLA.

As seen in Table 1, the normalized ΔH_m value (normalized by the weight of PLLA component), which is proportional to the degree of crystallinity ($X_{c,PLLA}$) of PLLA component, first increases and then decreases as the PDLLA content increases. This indicates that the incorporation of relatively small amount of PDLLA enhances the fraction of PLLA in the crystalline phase. This is partly due to the enhanced molecular mobility of PLLA with the incorporation of PDLLA component. As shown in Figures 1 and 2, the T_m value of PLLA slightly decreases with incorporation of PDLLA component. The equilibrium melting point (T_m^0) was estimated from Hoffman−Weeks linear extrapolation. Considering the α′-to-α phase transition upon heating, the samples crystallized above 110 °C, where the α-form crystals were predominantly produced, were only used to calculate the T_m^0 values. As seen in Table 1, the addition of PDLLA slightly depresses the T_m^0 value of PLLA. The higher the PDLLA content in the blend is, the more the depression of the T_m^0 of PLLA exhibits. With the incorporation of 75% PDLLA, the T_m^0 value of PLLA decreases by about 10 °C, which is consistent with the result reported previously.[27] The T_m^0 depression in the blends depends on both the composition and interaction parameter (χ). According to the Flory−Huggins equation,[37] it was estimated that the PLLA/PDLLA system exhibits a negative interaction parameter of −0.047. This indicates that the PLLA/PDLLA blends are thermodynamically miscible in the molten state. It should be noted that the interaction parameter between PLLA and PDLLA is larger than that of the PLLA/PVAc miscible blend (χ = −0.1),[23] which may suggest the lower extent of miscibility in the PLLA/PDLLA system. On the other hand, Jorda and Wilkes[38] have found that the prolonged aging below T_g can cause the phase separation of PLLA and PDLLA.

Spherulite Morphology. Figure 4 shows the POM micrographs of neat PLLA and its blends melt-crystallized at 140 °C. Neat PLLA shows the conventional Maltese-crossed spherulites with negative birefringence. However, in the PLLA/PDLLA 75/25 blend, PLLA spherulites show the coarse texture and irregular boundary, and the conventional Maltese-cross is disrupted. The PLLA/PDLLA 50/50 blend shows the ring-banded spherulites. In the PLLA/PDLLA 25/75 blend, the spherulites are too obscure to be clearly detected (data not shown). Previous studies have reported that PLLA (or PLLA segments) tends to form the ring-banded spherulites in the miscible or compatible blends [e.g., PLLA/a-PHB[21,22,39] and PLLA/ poly(ε-caprolactone)[40]] and the block copolymers (e.g., polystyrene-*b*-PLLA[40]). It is generally believed that the formation of banded spherulites is attributed to the lamellar twisting along the radial growth direction.[41,42] Therefore, it is reasonable to conclude that the PDLLA chains are trapped into the PLLA spherulites and disturb the regular orientation of crystalline

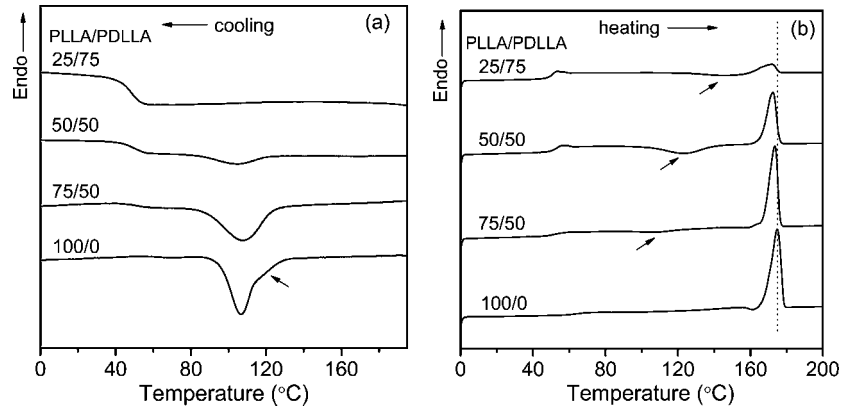

Figure 2. DSC curves of (a) nonisothermal melt-crystallization at a cooling rate of 2.5 °C/min and (b) subsequent heating scans at 10 °C/min for PLLA/PDLLA blends.

Table 1. Thermal Parameters of PLLA/PDLLA Blends Derived from DSC Analyses

			cold-crystallization			melt-crystallization		
PLLA/PDLLA	T_g (°C)	T_m^0 (°C)	T_c (°C)	ΔH_m (J/g PLLA)	T_m (°C)	T_c (°C)	ΔH_m (J/g PLLA)	T_m (°C)
100/0	55.0	192.0	107.8	42.0	175.0	106.6	42.5	174.3
75/25	53.1	189.2	121.1	52.7	174.7	107.7	51.9	173.2
50/50	51.4	185.6	130.5	56.1	172.5	104.7	57.0	172.3
25/75	49.5	182.8	145.1	26.4	171.4	N.P.[a]	31.9	170.7
0/100	47.1							

[a] N.P., no peak is observed.

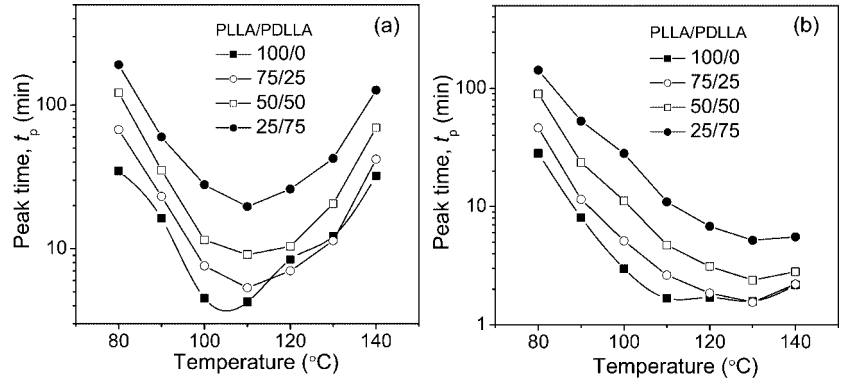

Figure 3. T_c dependence of DSC peak-times of isothermal (a) melt- and (b) cold-crystallization for PLLA/PDLLA blends.

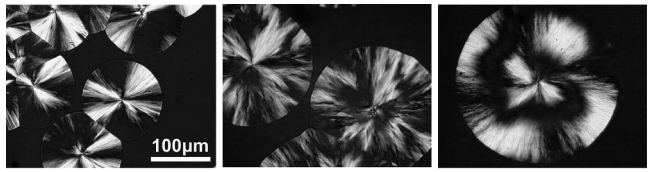

Figure 4. POM micrographs of PLLA/PDLLA blends melt-crystallized at 140 °C.

lamellae of PLLA. This further suggests that the PLLA and PDLLA components are miscible.

The radial growth rates (G) of PLLA spherulites for neat PLLA and it blends melt-crystallized at 140 °C were estimated from POM analysis. At $T_c = 140$ °C, the PLLA/PDLLA 75/25 blend shows a comparable G value ($G = 2.87$ μm/min) to neat PLLA ($G = 2.95$ μm/min). In the PLLA/PDLLA 50/50 and 25/75 blends, the G values decrease to 2.52 and 1.86 μm/min, respectively. In the miscible blends of crystalline/noncrystallizable polymers, the G value of crystallizable component is generally depressed by the mixing of amorphous component,[43,44] although blending with the noncrystalline low-molecular-weight polymers may increase the G value.[21,27] The depression of spherulite growth rate is usually caused by the dilution effect of the noncrystallizable component. Besides, as seen in Figure 4, the spherulite density slightly lowers as the PDLLA content increases. For the PLLA/PDLLA blends, the depression of the spherulite density and growth rate suggests that the crystallization rate of PLLA decreases upon blending with PDLLA, consistent with the aforementioned DSC data.

FTIR Spectra. The crystalline structure of PLLA in the blends crystallized at different T_cs was investigated by FTIR analysis. First, the T_c-dependent FTIR spectra of the PLLA/PDLLA blends were compared with those of neat PLLA. Figure 5 shows the (a) FTIR spectra and (b) corresponding second derivative spectra in 1810−1710 cm^{-1} region, ascribed to the carbonyl stretching vibration [ν(C═O)], for the PLLA/PDLLA 50/50 blend melt-crystallized at different T_cs. In the FTIR analysis, the second derivative spectra are usually used to identify the wavenumber and magnitude of the small bands or splitting bands. Figure 6 presents the FTIR spectra and corresponding second derivative spectra in 3075−2850 cm^{-1} region, attributed to the stretching vibration of CH_3 [$\nu(CH_3)$] and CH [ν(CH)], for (a) neat PLLA and (b) PLLA/PDLLA 50/50 blend melt-crystallized at different T_cs. The corresponding spectra of amorphous samples (indicated by "amor") were also shown in

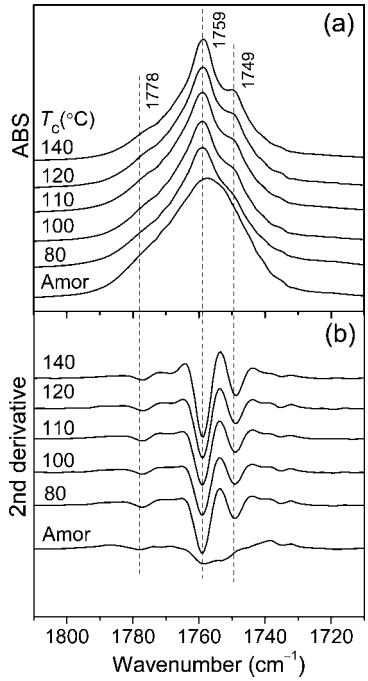

Figure 5. (a) FTIR spectra and (b) corresponding second derivative spectra in the wavenumber range of 1810−1710 cm^{-1} for PLLA/PDLLA 50/50 blend quenched (indicated by "amor") and melt-crystallized at T_c = 80−140 °C.

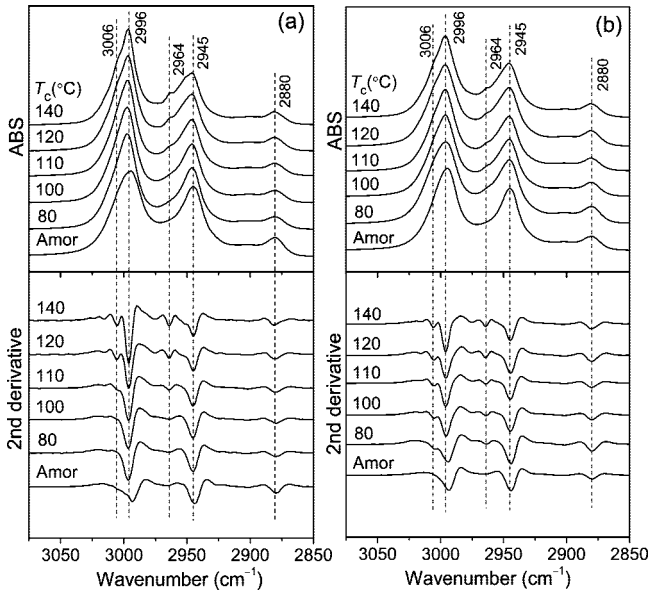

Figure 6. FTIR spectra and corresponding second derivative spectra in the wavenumber range of 3075−2850 cm^{-1} for (a) neat PLLA and (b) PLLA/PDLLA 50/50 blend quenched (indicated by "amor") and melt-crystallized at T_c = 80−140 °C.

Figures 5 and 6 for comparison. At T_c < 80 or >140 °C, the crystallization of PLLA/PDLLA blends is extremely slow, and thus the samples were only crystallized at the T_c region of 80−140 °C in this study. The assignments of FTIR bands are based on the results of Kister et al.[45] The amorphous samples (prepared by quenching) of PLLA, PDLLA, and PLLA/PDLLA blends with various compositions show the nearly identical FTIR spectra (data not shown). This can be expected because PLLA and PDLLA are almost the same from a spectroscopic viewpoint. Therefore, the spectral difference between the crystallized PLLA and PLLA/PDLLA blends can be considered to be due to the effects of crystalline structure.

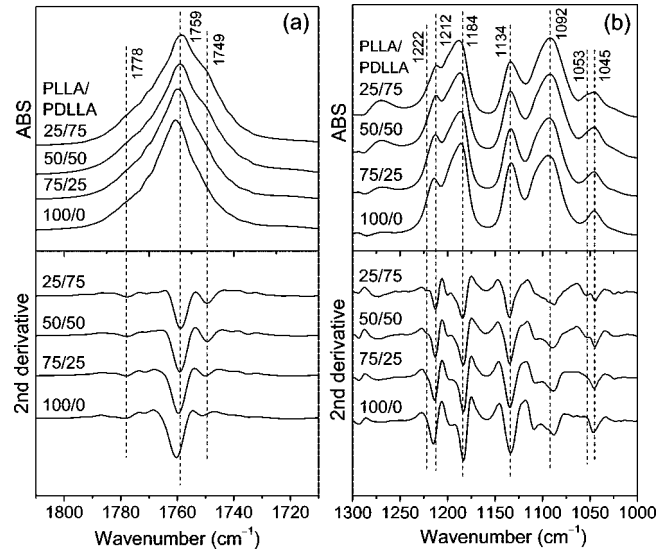

Figure 7. FTIR spectra and corresponding second derivative spectra in the wavenumber ranges of (a) 1810−1710 and (b) 1300−1000 cm^{-1} for PLLA/PDLLA blends with different compositions melt-crystallized at T_c = 80 °C.

As reported previously,[7,8] in the case of neat PLLA, the splitting band at 1749 cm^{-1} only appears in the spectrum of the α-form crystals, which are predominantly developed at high T_c (>110 °C), but absent in that of the α′-form crystals produced at low T_c (<100 °C) (Figure S1). As the T_c value increases from 80 to 140 °C, the ν(C═O) band of PLLA shifts slightly to lower-wavenumber side by 1−2 cm^{-1}, corresponding to the phase transformation from the α′- to α-form crystals (Figure S1). As shown in Figure 6a, the splitting bands of $\nu_{as}(CH_3)$ at 3006 cm^{-1} and $\nu_s(CH_3)$ at 2964 cm^{-1} appear in the spectrum of neat PLLA crystallized at high T_c (>110 °C), but are absent in that crystallized at low T_c (<100 °C). A very similar trend is observed in other regions of the FTIR spectra. As seen in Figures S2a and S3a, the splitting bands of $\delta_s(CH_3)$ at 1382 cm^{-1}, ν_{as}(C−O−C) + $r_{as}(CH_3)$ at 1222 cm^{-1}, and ν(C−CH_3) at 1053 cm^{-1} appear in the spectrum of neat PLLA crystallized at high T_c, but disappear in that crystallized at low T_c. All the splitting bands, caused by the intramolecular or intermolecular interactions in the crystalline phase,[46,47] are characteristics of the α-form PLLA, rather than its α′-counterpart.[7,8] These FTIR data is consistent with the previously reported result that the PLLA α- and α′-form crystals are predominantly developed at high and low T_c, respectively.[7,8]

However, as seen in Figure 5, 6b, S2b, and S3b, the splitting bands at 1749, 3006, 2964, 1382, 1222, and 1053 cm^{-1}, all of which are characteristics of the α-form PLLA, appear in the spectrum of the PLLA/PDLLA 50/50 blend crystallized over the T_c range of 80−140 °C. The peak wavenumber of ν(C═O) band locates at 1759 cm^{-1} for PLLA/PDLLA 50/50 blend crystallized at various T_cs, and no wavenumber shift is observed as T_c changes. These results suggest that the PLLA α-form crystals, rather than their α′-counterparts, are predominantly developed in the PLLA/PDLLA 50/50 blend crystallized at T_c = 80−140 °C. Besides, these splitting bands become more apparent with T_c, indicating the increase in the α-form fraction with T_c.

The effects of blend composition on the crystalline structure of PLLA were further investigated by FTIR analysis. Figure 7 shows the FTIR spectra and corresponding second derivative spectra in (a) 1810−1710 and (b) 1300−1000 cm^{-1} ranges for the blends with different compositions crystallized at 80 °C. As seen in Figure 7, at T_c = 80 °C, the splitting bands at 1749, 1222, and 1053 cm^{-1}, characteristics of the α-form PLLA, are

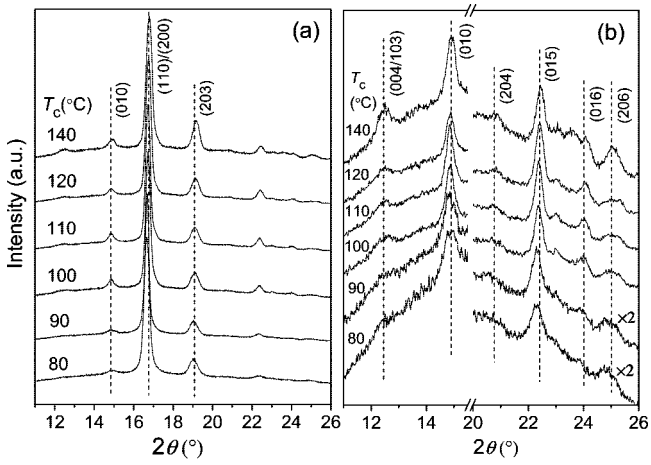

Figure 8. (a) WAXD patterns and (b) enlarged profiles for small peaks of PLLA/PDLLA 50/50 blend melt-crystallized at T_c = 80−140 °C.

present in the blends with PDLLA fraction (f_{DL}) ≥ 0.50, but disappear in those with f_{DL} ≤ 0.25. The similar trend was also detected for the splitting bands of $\nu(CH_3)$ and $\delta(CH_3)$ modes (data not shown). These results indicate that, at T_c = 80 °C, the α′- and α-form crystals of PLLA are predominantly formed in the blends with f_{DL} ≤ 0.25 and ≥0.50, respectively. At T_c = 100 °C, these splitting bands are observed in the spectra of the blends with f_{DL} ≥ 0.25, but absent in that of the neat PLLA (Figure S4). However, as T_c is increased to 120 °C, all these splitting bands appear in the spectra of the neat PLLA and its blend samples (Figure S5). From these results, it can be concluded that the crystal modifications of PLLA is considerably influenced by the blend composition. As the PDLLA composition increases, the critical temperature for the generation of the PLLA α′- and α-form crystals decreases.

WAXD Patterns. The crystalline structure of PLLA/PDLLA blends crystallized at different T_cs was further investigated by WAXD analysis. Figure 8 shows the WAXD patterns of the PLLA/PDLLA 50/50 blend crystallized at T_c = 80−140 °C. For clarity, the profiles of the weak reflections are enlarged in panel b of Figure 8. As reported previously,[8,9] with an increase in T_c, the two strongest WAXD reflections of neat PLLA, that is, (110)/(200) and (203), shift to higher 2θ side, corresponding to the transition from α′- to α-form crystals. Besides, the α′-form PLLA exhibits a characteristic reflection at 2θ = ∼24.5°, but two reflections, that is, (016) and (206), appear in this 2θ range for the α-form PLLA.[8,11]

As seen in Figure 8, for the PLLA/PDLLA 50/50 blend crystallized at T_c = 80−140 °C, the characteristic reflection of the α′-form (2θ = ∼24.5°) is absent and two reflections of the α-form crystals, that is, (016) and (206), are observed at 2θ = 23−26°. The (110)/(200) reflections of the PLLA/PDLLA 50/50 blend crystallized at T_c = 80−140 °C locate at higher 2θ (16.7−16.8°) than that of the PLLA α′-form crystals (∼16.5°). These imply that the α-form crystals of PLLA are mainly developed in the PLLA/PDLLA 50/50 blend crystallized at the investigated T_c region. In the PLLA/PDLLA 75/25 blend, the samples crystallized at T_c > 90 °C and T_c < 90 °C show the typical WAXD profiles of the PLLA α-form and α′-form crystals, respectively (Figure S6). In the PLLA/PDLLA 25/75 blend, the WAXD patterns of the samples crystallized at T_c = 80−140 °C exhibit the characteristic reflections of the α-form PLLA (data not shown). These WAXD results agree well with the FTIR data and further suggest that the critical T_c for generating the PLLA α′- and α-form crystals, which are respectively ∼110, ∼90, and ∼80 °C for neat PLLA, PLLA/PDLLA 75/25, and PLLA/PDLLA 50/50 samples, decreases as the PDLLA fraction increases.

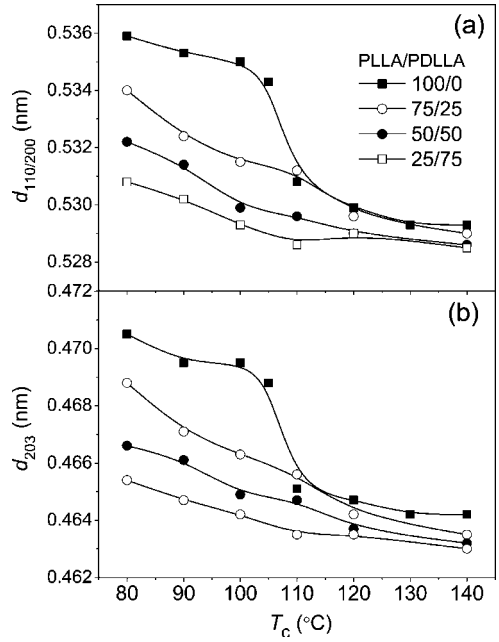

Figure 9. T_c dependence of lattice spacings for (a) (110)/(200) and (b) (203) reflections of PLLA in the PLLA/PDLLA blends with different compositions.

On the basis of the WAXD results, the lattice spacings (d) of the (110)/(200) and (203) diffractions, $d_{110/200}$ and d_{203}, were estimated by the Bragg equation. Figure 9 shows the T_c dependence of $d_{110/200}$ and d_{203} for neat PLLA and its blends. For neat PLLA, the values of $d_{110/200}$ and d_{203} decrease abruptly with T_c at ∼110 °C, indicating that the α-form PLLA has slightly smaller unit cell dimensions than its α′-counterpart. For the PLLA/PDLLA blends, the values of $d_{110/200}$ and d_{203} also decrease with T_c, but the extent of decrease is much smaller compared to that of the neat PLLA. It can be estimated from Figure 9 that the α-form content in all the samples increases with T_c, and at the identical T_c, the α-form fraction increases with an increase in the PDLLA composition.

Thermodynamic and Kinetic Considerations. Among the different modifications of a given polymorphic polymer, there is usually a polymorph which is thermodynamically the most stable, corresponding to the crystal formed under the usual crystallization conditions. The formation of a stable phase is generally thermodynamically controlled. Other less stable modifications can be considered as the metastable phases at a specific temperature and pressure.[48] The metastable phases are considered to fall into one of the multiple local free energy minima in Gibbs free energy profile and will ultimately transform into the thermodynamic state of global free energy minima under the appropriate conditions. Previous studies[8−11] have reported that the PLLA α′-form transforms into its α-counterpart upon heating or annealing at elevated temperatures. Therefore, the α′- and α-form crystals can be considered as the metastable and stable phases of PLLA, respectively.

All of the DSC, FTIR, and WAXD results indicate that the crystalline structure of PLLA is influenced by the miscible blending with PDLLA, and the formation of the PLLA α-form crystals is facilitated in the blend systems. This is caused by the effects of blending on the thermodynamic and kinetics environments of PLLA crystallization. From the viewpoint of thermodynamics, the depression of T_g and T_m^0 upon blending will shift the crystallization temperature window to low-temperature side and thus decrease the critical T_c for the generation of the α′- and α-form crystals. In the other experiment, we have found that, for the blend sample of the low-

molecular-weight PLLA (M_n = 15 kDa) with PDLLA, both of which have almost the same T_g (~47 °C), the similar effects of blending on crystal modifications of PLLA were observed (data not shown). Thus, it is considered that the effect of T_g of the PLLA/PDLLA blends on the polymorphic behavior of PLLA can be neglected. On the other hand, the change in the T_m^0 value of PLLA upon blending with PDLLA is relatively small. With incorporation of 50 wt % PDLLA, the T_m^0 value of PLLA decreases by ~6 °C, while the critical T_c for the generation of PLLA α′- and α-form crystals decreases by ~30 °C (from ~110 to ~80 °C). Therefore, it is reasonably concluded that, aside from the thermodynamic effect, the crystallization kinetics could be a crucial contribution for the change of crystalline structure upon blending.

According to the metastable theory,[48] the formation of a metastable phase is usually due to the kinetic effects that provide a favorable pathway for the polymer to fall into the local free energy minimum. Previous studies have evidenced that the formation of the metastable α-form crystals in s-PS[18] and the metastable β-form crystals in poly(butylene adipate) (PBA),[49] both produced at relatively lower T_c, is ascribed to the kinetic contribution. Accordingly, it is proposed that the formation of the metastable α′-form crystals in PLLA could be kinetically controlled, while that of the stable α-form is thermodynamically driven. The incorporation of PDLLA component considerably affected the crystallization kinetics of PLLA, which could cause the change in crystalline structure. The effects of miscible blending on the crystalline structure of PLLA can be ascribed to two main factors, that is, the lowered T_m^0 and decreased crystallization rate, which is similar to the case of s-PS.[18]

Conclusions

The crystallization kinetics and crystalline structure of PLLA in the PLLA/PDLLA blends have been studied. PLLA and PDLLA are miscible at all compositions. Because of the dilution effect, the crystallization rate of PLLA decreases and the T_m^0 value of PLLA is slightly depressed with the incorporation of PDLLA. Both the FTIR and WAXD results suggest that the crystalline structure of PLLA is affected by the miscible blending and the formation of the PLLA α-form crystals is favored in the blend systems. The critical T_c for the formation of the α′- and α-form crystals of PLLA decreases significantly upon blending with the noncrystallizable PDLLA. With combination of the DSC, FTIR, and WAXD results, it was proposed that the formation of metastable α′-form and thermally stable α-form crystals in PLLA are kinetically and thermodynamically driven, respectively. This study has explained the crystallization mechanism of the α′- and α-form crystals to certain extent and also provided a convenient method to regulate the crystalline structure of PLLA.

Acknowledgment. We thank Prof. Minoru Sakurai for the use of FTIR instrument and Dr. Kazue Ueda of Unitika Co. Ltd. (Kyoto, Japan) for kindly supplying the PLLA sample.

Supporting Information Available: Figures showing FTIR spectra and WAXD patterns of PLLA/PDLLA blends crystallized at different T_cs. This material is available free of charge via the Internet at http://pubs.acs.org.

References and Notes

(1) Nair, L. S.; Laurencin, C. T. *Prog. Polym. Sci.* **2007**, *32*, 762–798.
(2) Lim, L.-T.; Auras, R.; Rubino, M. *Prog. Polym. Sci.* **2008**, *33*, 820–852.
(3) De Santis, P.; Kovacs, J. *Biopolymers* **1968**, *6*, 299–306.
(4) Sasaki, S.; Asakura, T. *Macromolecules* **2003**, *36*, 8385–8390.
(5) Eling, B.; Gogolewski, S.; Pennings, A. J. *Polymer* **1982**, *23*, 1587–1593.
(6) Cartier, L.; Okihara, T.; Ikada, Y.; Tsuji, H.; Puiggali, J.; Lotz, B. *Polymer* **2000**, *41*, 8909–8919.
(7) Zhang, J.; Duan, Y.; Sato, H.; Tsuji, H.; Noda, I.; Yan, S.; Ozaki, Y. *Macromolecules* **2005**, *38*, 8012–8021.
(8) Pan, P.; Kai, W.; Zhu, B.; Dong, T.; Inoue, Y. *Macromolecules* **2007**, *40*, 6898–6905.
(9) Kawai, T.; Rahman, N.; Matsuba, G.; Nishida, K.; Kanaya, T.; Nakano, M.; Okamoto, H.; Kawada, J.; Usuki, A.; Honma, N.; Nakajima, K.; Matsuda, M. *Macromolecules* **2007**, *40*, 9463–9469.
(10) Yasuniwa, M.; Sakamo, K.; Ono, Y.; Kawahara, W. *Polymer* **2008**, *49*, 1943–1951.
(11) Pan, P.; Zhu, B.; Kai, W.; Dong, T.; Inoue, Y. *Macromolecules* **2008**, *41*, 4296–4304.
(12) Di Lorenzo, M. L. *Eur. Polym. J.* **2005**, *41*, 569–575.
(13) Corradini, P.; Guerra, G. *Adv. Polym. Sci.* **1992**, *100*, 183–217.
(14) Gan, Z.; Kuwabara, K.; Abe, H.; Iwata, T.; Doi, Y. *Polym. Degrad. Stab.* **2005**, *87*, 191–199.
(15) Mathieu, C.; Thierry, A.; Wittmann, J. C.; Lotz, B. *J. Polym. Sci., Part B: Polym. Phys.* **2002**, *40*, 2504–2515.
(16) Miyazaki, T.; Takeda, Y.; Akasaka, M.; Sakai, M.; Hoshiko, A. *Macromolecules* **2008**, *41*, 2749–2753.
(17) Sun, Y.; Li, H.; Huang, Y.; Chen, E.; Zhao, L.; Gan, Z.; Yan, S. *Macromolecules* **2005**, *38*, 2739–2743.
(18) Woo, E. M.; Sun, Y. S.; Yang, C. P. *Prog. Polym. Sci.* **2001**, *26*, 945–983.
(19) Lee, K.-H.; Givens, S. R.; Snively, C. M.; Chase, B.; Rabolt, J. F. *Macromolecules* **2008**, *41*, 3144–3148.
(20) Li, Y.; Iwakura, Y.; Shimizu, H. *Macromolecules* **2008**, *41*, 3396–3400.
(21) Ohkoshi, I.; Abe, H.; Doi, Y. *Polymer* **2000**, *41*, 5985–5992.
(22) Focarete, M. L.; Ceccorulli, G.; Scandola, M.; Kowalczuk, M. *Macromolecules* **1998**, *31*, 8485–8492.
(23) Park, J. W.; Im, S. S. *Polymer* **2003**, *44*, 4341–4354.
(24) Zhang, G. B.; Zhang, J. M.; Wang, S. G.; Shen, D. Y. *J. Polym. Sci., Part B: Polym. Phys.* **2003**, *41*, 23–30.
(25) Meaurio, E.; Zuza, E.; Sarasua, J.-R. *Macromolecules* **2005**, *38*, 1207–1215.
(26) Hu, Y.; Hu, Y. S.; Topolkaraev, V.; Hiltner, A.; Baer, E. *Polymer* **2003**, *44*, 5711–5720.
(27) Tsuji, H.; Ikada, Y. *Polymer* **1996**, *37*, 595–602.
(28) Ren, J.; Adachi, K. *Macromolecules* **2003**, *36*, 5180–5186.
(29) Abe, H.; Harigaya, M.; Kikkawa, Y.; Tsuge, T.; Doi, Y. *Biomacromolecules* **2006**, *6*, 457–467.
(30) Baratian, S.; Hall, E. S.; Lin, J. S.; Xu, R.; Runt, J. *Macromolecules* **2001**, *34*, 4857–4864.
(31) Huang, J.; Lisowski, M. S.; Runt, J.; Hall, E. S.; Kean, R. T.; Buehler, N.; Lin, J. S. *Macromolecules* **1998**, *31*, 2593–2599.
(32) Yuryev, Y.; Wood-Adams, P.; Heuzey, M.-C.; Dubois, C.; Brisson, J. *Polymer* **2008**, *49*, 2306–2320.
(33) Tsuji, H.; Tezuka, Y.; Saha, S. K.; Suzuki, M.; Itsuno, S. *Polymer* **2005**, *46*, 4917–4927.
(34) Urayama, H.; Moon, S.-I.; Kimura, Y. *Macromol. Mater. Eng.* **2003**, *288*, 137–143.
(35) Kang, S.; Zhang, G.; Aou, K.; Hsu, S. L.; Stidham, H. D.; Yang, X. *J. Chem. Phys.* **2003**, *118*, 3430.
(36) Gordon, M.; Taylor, J. S. *J. Appl. Chem.* **1952**, *2*, 493–500.
(37) Flory P. J. *Principles of Polymer Chemistry*; Cornell University Press: New York, 1953.
(38) Jorda, R.; Wilkes, G. L. *Polym. Bull.* **1998**, *20*, 479–485.
(39) Xu, J.; Guo, B. H.; Zhou, J.-J.; Li, L.; Wu, J.; Kowalczuk, M. *Polymer* **2005**, *46*, 9176–9185.
(40) Chao, C.-C.; Chen, C.-K.; Chiang, Y.-W.; Ho, R.-M. *Macromolecules* **2008**, *41*, 3949–3956.
(41) Schultz, J. M. *Polymer* **2003**, *44*, 433–441.
(42) Xu, J.; Guo, B.-H.; Zhang, Z.-M.; Zhou, J.-J.; Jiang, Y.; Yan, S.; Li, L.; Wu, Q.; Chen, G.-Q.; Schultz, J. M. *Macromolecules* **2004**, *37*, 4118–4123.
(43) Abe, H.; Doi, Y.; Satkowski, M. M.; Noda, I. *Macromolecules* **1994**, *27*, 50–54.
(44) Wang, C.; Lin, C.-C.; Chu, C.-P. *Macromolecules* **2006**, *39*, 9267–9277.
(45) Kister, G.; Cassanas, G.; Vert, M. *Polymer* **1998**, *39*, 267–273.
(46) Aou, K.; Hsu, S. L. *Macromolecules* **2006**, *39*, 3337–3344.
(47) Meaurio, E.; Zuza, E.; López-Rodríguez, N.; Sarasua, J. R. *J. Phys. Chem. B* **2006**, *110*, 5790–5800.
(48) Keller, A.; Cheng, S. Z. D. *Polymer* **1998**, *39*, 4461–4487.
(49) Gan, Z.; Kuwabara, K.; Abe, H.; Iwata, T.; Doi, Y. *Biomacromolecules* **2004**, *5*, 371–378.

MA8024943